



**rijksuniversiteit  
 groningen**

# Mimicking in vivo phase 1 metabolism of pharmaceuticals by Electrochemistry

Bachelor Research Project Pharmacy

Name: Annemay Breman

Student number: S3985989

Date: 23/06/2022

Coordinator: H.P. Permentier

## Abstract

Early assessment of phase 1 metabolic pathways can help to identify in vivo metabolites, thereby giving an insight in which drug candidates to eliminate before entering a loathsome clinical trial. The aim of this study was to investigate whether electrochemistry (EC) coupled off-line with liquid chromatography combined with mass spectrometry (LC-MS) is competent to mimic in vivo phase 1 metabolism of pharmaceuticals. With the aim of doing this, several pharmaceuticals were oxidized in an electrochemical cell under various conditions followed by detection by LC/MS to look whether known in vivo oxidative metabolites were formed. In the present study, fifteen distinctive pharmaceuticals were used as drug compounds to study the formation of potential in vivo phase 1 metabolites. The in vivo phase 1 metabolism of seven pharmaceuticals was successfully mimicked whereas this was not the case for six other pharmaceuticals. For the last two pharmaceuticals, only one of the two expected oxidative metabolites was detected. The catalytic working of hydrogen peroxide combined with a platinum electrode was found to have a major effect on oxygen-insertion reactions and thereby on hydroxylation, N-oxidation and sulfoxidation. Whereas the cell potential did not have a significant influence on the metabolite formation.

## Contents

|  |    |
|--|----|
| Abstract .....   | 2  |
| Introduction.....  | 4  |
| Materials and Methods .....  | 9  |
| Chemicals.....   | 9  |
| Preparation of samples .....   | 9  |
| Oxidation of samples in electrochemical cell.....                            | 9  |
| LC-MS analysis of collected samples .....                                    | 10 |
| Data analysis .....  | 11 |
| Results and Discussion .....   | 13 |
| The different conditions.....  | 13 |
| Pharmaceuticals without oxidative metabolites.....                           | 13 |
| Pharmaceuticals with dealkylated in vivo metabolites.....                    | 14 |
| Pharmaceuticals with hydroxylated in vivo metabolites .....                  | 16 |
| Pharmaceuticals with dealkylated and hydroxylated in vivo metabolites.....   | 17 |
| Pharmaceuticals with dealkylated and N-/S-oxidated in vivo metabolites ..... | 18 |
| Conclusion .....   | 21 |
| References.....  | 22 |

## Introduction

The demand for medicine is increasing due to the ascending average age of people, the discovery of new diseases and the development of drug resistance. Fortunately, the pharmaceutical industry is entering a new era in medicine development thanks to an advancement in science and technology, making it possible to develop such high numbers of drugs. However, before a drug enters the market, it must be evaluated throughout various stages in a clinical trial, which is loathsome to do for such high numbers of drug candidates. To reduce the amount of drug candidates entering a clinical trial, drugs candidates can be eliminated beforehand based on their pharmacokinetics. One stage of pharmacokinetics which is considered to be important is metabolism, since it can have a critical role in pharmacological- as well as toxicological effects in humans. Therefore, early assessments of metabolic pathways in humans can help to get an insight in metabolites and eliminate drug candidates based on this information [1]. With the aim of doing this, new analytical techniques competent to do early, quick, and cheap assessment of drug metabolism must be assessed.

Drugs are seen as xenobiotics by the body, meaning that once the human body detects a drug it wants to eliminate this. Metabolism makes it possible for the human body to remove these xenobiotics via the kidneys in the urine. Drug metabolism mainly takes place in the liver and starts with an initial phase (Phase 1), which is possibly followed by a second phase (Phase 2) and a potential third phase (Phase 3) [2]. During Phase 1 metabolism, drugs are enzymatically bio transformed into active or inactive compounds with the goal to increase the polarity of the compound. Subsequently, Phase 2 metabolism enzymatically conjugates the compound with an endogenous compound, thereby making it more water-soluble and inactive, if necessary, so that the product can be excreted by the body. Phase 3 metabolism occurs when the product of Phase 2 cannot passively pass the membrane into the urine and thus must be actively transported by ABC transporters from one side of the cell membrane to the other [3].

The major group of enzymes active during Phase 1 metabolism are part of the Cytochrome P450 (CYP450) superfamily. Members of this family, also known as the CYPs, are capable of bio transforming drugs into inactive and more water-soluble products, thereby promoting excretion by the kidney in the urine and/or the liver in the bile. CYP450s are attached to the endoplasmic reticulum or mitochondria of mainly the liver via a short N-terminal membrane anchoring segment. The amino acids present in the N-terminal anchor are hydrophobic thereby enhancing the interaction with the hydrophobic ER membrane [4]. Figure 1 shows a schematic

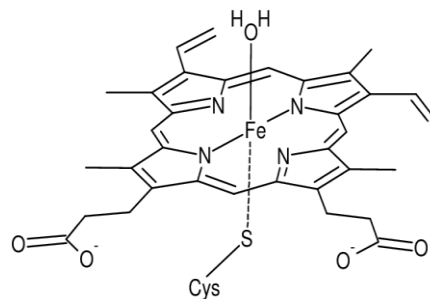


Figure 1: Chemical structure of CYP450 in resting state [6].

structural formula of a CYP450 enzyme in resting state. In the catalytic site of the enzyme a heme iron is located that is tethered to the protein by a sulfur atom of a cysteine thiolate. On the distal axial coordination position a water molecule is attached to the heme iron leading to a low-spin state of the heme iron thereby making the enzyme inactive. Even though the heme iron in Figure 1 is located in the center of the enzyme, it is still based near the enzyme surface, making it possible for substrates to bind to the hydrophobic pocket adjacent to the active site [5]. When the substrate has bound to the hydrophobic pocket, the active site will undergo a conformational change, often displacing the water molecule bound to the heme iron. Due to this, the heme iron will go from a low-spin state to a high-spin state, making the enzyme active and ready to catalyze a wide variety of reactions [4]. Examples of oxidation reactions include

N-oxidation, C-oxidation, aliphatic hydroxylation, aromatic hydroxylation, sulfoxidation, N-dealkylation, O-dealkylation and epoxidation. All these reactions make the drug more polar and sometimes inactive [3].

Figure 2 shows a schematic representation of the catalytic cycle of the CYP450 enzyme during a hydroxylation reaction. Binding of the substrate (RH) to the CYP450 enzyme will displace the water molecule leaving a high-spin state  $\text{Fe}^{3+}$ -heme. Subsequently, there will be electron transfer from NAD(P)H via a CYP reductase protein resulting in  $\text{Fe}^{2+}$ -heme. The formed ferrous heme center will bind to molecular oxygen leading to a dioxygen adduct in the now formed oxy- $\text{Fe}^{2+}$ -heme. This adduct will be reduced again via a CYP reductase inhibitor giving a  $\text{Fe}^{2+}$ -peroxy species, which is easily protonated twice since it is a good base. Due to the double protonation, one water molecule is released, thereby forming P450 Compound 1. This species is known to be highly reactive and can bind an oxygen atom to the substrate, making the substrate more hydrophilic, thereby promoting excretion by the body. After oxidation, a water molecule returns to bind to the distal coordination position of the heme iron, returning the enzyme to its low-spin and thus resting state. When a new substrate binds again to the hydrophobic pocket of the enzyme, this cycle will be repeated [5].

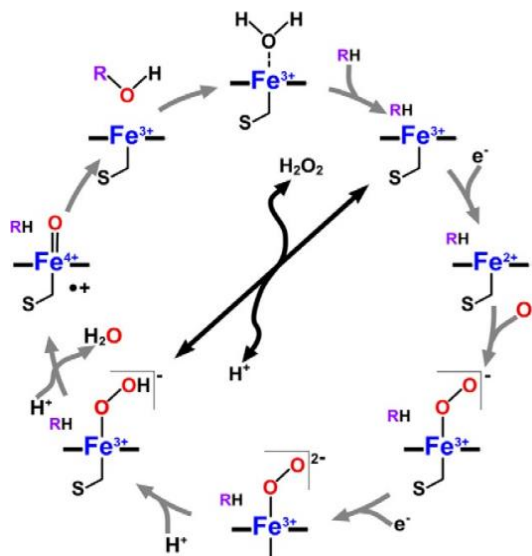


Figure 2: schematic representation of the catalytic cycle of the CYP450 [7].

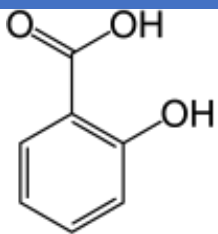
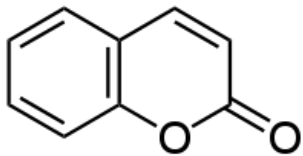
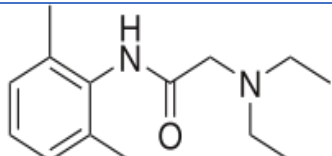
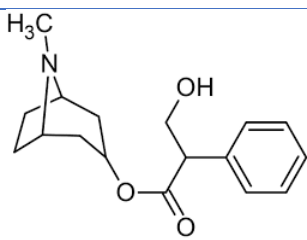
After oxidation, a water molecule returns to bind to the distal coordination position of the heme iron, returning the enzyme to its low-spin and thus resting state. When a new substrate binds again to the hydrophobic pocket of the enzyme, this cycle will be repeated [5]. The different oxidation reactions all rely on the same principle explained above; an oxygen atom is introduced to the drug, making it more polar. With N-oxidation, C-oxidation, aromatic hydroxylation, aliphatic hydroxylation, epoxidation and sulfoxidation no other chemical reaction takes place after the oxygen atom has covalently bound to the drug with a single- or double bond. Yet, with N-dealkylation and O-dealkylation a leaving group is created after the oxygen atom has bound to the drug. Subsequently, this group, consisting of carbon atoms, hydrogen atoms and an oxygen atom, will leave the molecule resulting in the dealkylated form [8].

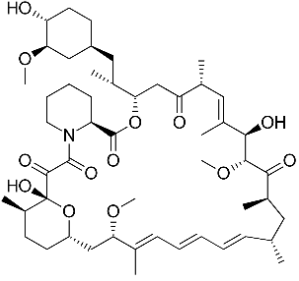
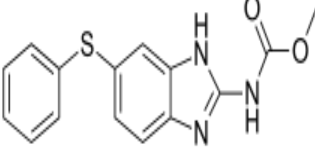
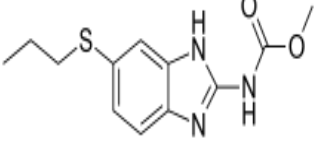
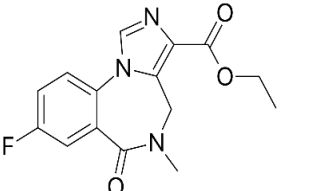
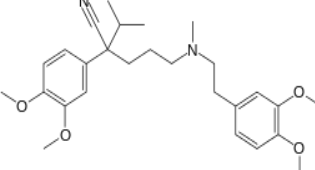
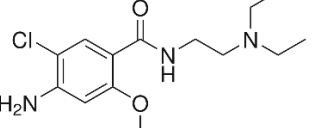
Electrochemistry is an electrochemical technique used to study electron movement in either oxidation reactions or reduction reactions at an electrode surface in an electrochemical cell. There are two types of electrochemical cells, namely the galvanic cell and electrolytic cell. The galvanic cell obtains energy from spontaneous redox reactions happening at the electrode, while the electrolytic cells require an external energy source for the redox reactions to happen. Since phase 1 metabolism of drugs does not happen spontaneously but is instead enzymatically driven, an electrolytic cell is chosen for this study, making it possible to mimic the CYP-induced metabolism of drugs [9]. After the analyte is oxidized in the electrochemical cell, it can be analyzed by various analytical methods giving information about the nature and properties of the compound contained in the cell. Mass spectrometry is a popular analytical technique since it provides both quantitative and qualitative data about the analyte. Combining electrochemistry directly with mass spectrometry, also called on-line EC-MS, was introduced around 20 years ago and was quickly found out to offer interesting information about oxidative products of analytes. With on-line EC-MS, the electrochemical cell is coupled with electrospray ionization (ESI), leading to the formation of ions from the analyte which can subsequently be analyzed in the mass spectrometer. Despite the promising set-up, no further information, except that from the mass spectrometer, is available about the oxidation products. Accordingly, High-performance liquid chromatography (HPLC) can be combined with the EC-MS

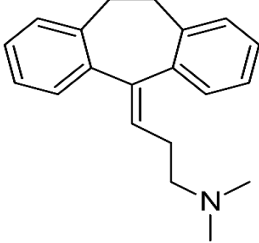
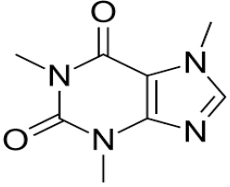
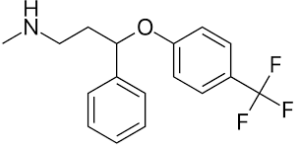
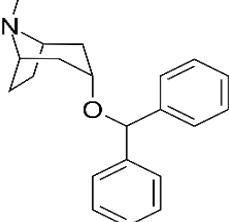
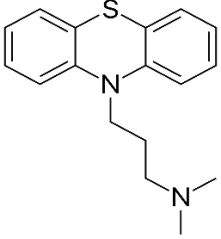
resulting in an EC/LC/MS setup. Besides information being obtained about oxidative products by the MS, now also valuable information about the polarity of the oxidative products is obtained through the LC. Besides this, the potential multiple oxidative products are also separated due to the column, before entering the MS, making it less complicated to detect oxidative products [10].

The objective of this study is to mimic in vivo phase 1 metabolism of a panel of pharmaceuticals via electrochemistry coupled off-line with LC/MS. For this study, a wide variety of pharmaceuticals is chosen with different chemical structures, pharmacological effects, and in vivo oxidative metabolites. This wide variety of pharmaceuticals makes it possible to identify differences between expected oxidation reactions and the extent to which electrochemistry can mimic these.

Table 1: representation of studied pharmaceuticals with their belonging in vivo phase 1 metabolites and type of oxidation reaction.

| Pharmaceutical  | In vivo metabolite  | Oxidation reaction               |
|---|---|----------------------------------|
| <br>Salicylic acid | 2,5-dihydroxybenzoic acid [11]  | Aromatic hydroxylation           |
| <br>Coumarin      | 7-hydroxycoumarin [12]  | Aromatic hydroxylation           |
| <br>Lidocaine    | 1.MEGX (mono-ethyl-glycine xylidide) [13]<br>2.GX (glycine xylidide) [13] | N-dealkylation<br>N-dealkylation |
| <br>Atropine     | Noratropine [14]  | N-dealkylation                   |

|   |   |                         |
|---|---|-------------------------|
|    |   |                         |
| Rapamycin   | 1.41-O-desmethyl-rapamycin [15]             | O-dealkylation          |
|   | 2.Hydroxy rapamycin (unknown position) [15] | Aliphatic hydroxylation |
|    |   |                         |
| Fenbendazole  | 4-Hydroxyfenbendazole [16]                  | Aromatic hydroxylation  |
|    |   |                         |
| Albendazole   | 8-Hydroxyalbendazole [16]                   | Aliphatic hydroxylation |
|   |   |                         |
| Flumazenil  | N-demethylated flumazenil [17]              | N-dealkylation          |
|  |   |                         |
| Verapamil   | Norverapamil [18]                           | N-dealkylation          |
|  |   |                         |
| Metoclopramide  | 1.N-deethylated metoclopramide [19]         | N-dealkylation          |
|   | 2.mono-oxygenated metoclopramide [19]       | N-oxidation             |

|  |   |   |
|--|---|---|
|  <p>Amitriptyline</p> | <p>1.Nortriptyline [20]</p> <p>2.10-hydroxy amitriptyline [20]</p>      | <p>N-dealkylation</p> <p>Aromatic hydroxylation</p> |
|  <p>Caffeine</p>      | <p>1,7-dimethylxanthine [21]</p>  | <p>N-dealkylation</p>                               |
|  <p>Fluoxetine</p>    | <p>Norfluoxetine [22]</p>   | <p>N-dealkylation</p>                               |
|  <p>Benztropine</p>  | <p>1.N-desmethylbenztropine [23]</p> <p>2.4-Hydroxybenztropine [23]</p> | <p>N-dealkylation</p> <p>Aromatic hydroxylation</p> |
|  <p>Promazine</p>   | <p>1.N-desmethylpromazine [24]</p> <p>2.Promazine sulfoxide [24]</p>    | <p>N-dealkylation</p> <p>Sulfoxidation</p>          |



## Materials and Methods

### Chemicals

The pharmaceuticals used:

Benzotropine ( $C_{21}H_{25}NO$ ), caffeine ( $C_8H_{10}N_4O_2$ ), fenbendazole ( $C_{15}H_{13}N_3O_2S$ ), amitriptyline hydrochloride ( $C_{20}H_{23}N \cdot HCl$ ), metoclopramide hydrochloride ( $C_{14}H_{22}ClN_3O_2 \cdot HCl$ ), albendazole ( $C_{12}H_{15}N_3O_2S$ ), salicylic acid ( $C_7H_6O_3$ ), promazine hydrochloride ( $C_{17}H_{20}N_2S \cdot HCl$ ), atropine ( $C_{17}H_{23}NO_3$ ), coumarin ( $C_9H_6O_2$ ) and lidocaine ( $C_{14}H_{22}N_2O$ ) were obtained from Sigma-Aldrich. Rapamycin ( $C_{51}H_{79}NO_{13}$ ) was obtained from Innocore Pharma. Fluoxetine hydrochloride ( $C_{17}H_{18}F_3NO \cdot HCl$ ) was obtained from TCI. Lastly, it was unknown from which flumazenil ( $C_{15}H_{14}FN_3O_3$ ) and verapamil hydrochloride ( $C_{27}H_{38}N_2O_4 \cdot HCl$ ) were purchased.

Other chemicals used as solvents, mobile phase, reagents:

Methanol ( $CH_3OH$ ) and acetonitrile ( $C_2H_3N$ ) were obtained from Biosolve. Formic acid (FA;  $H_2CO_2$ ) was obtained from Fluka. Dimethyl sulfoxide (DMSO;  $(CH_3)_2SO$ ) and hydrogen peroxide 30% ( $H_2O_2$ ) were ordered from Sigma-Aldrich. Ultrapure water was purified using a Mili-Q purification system.

### Preparation of samples

All 15 pharmaceuticals used were weighed out and were dissolved in methanol till a concentration of 10 mM was achieved in 10 mL. Except for rapamycin and verapamil, for these pharmaceuticals an end concentration of 1 mM in 10 mL was formed, since not enough pharmaceutical was available to get a concentration of 10 mM. An example calculation for 10 mM in 10 mL:

Molar concentration (M) = amount of substance (mole)/ Volume (L)

Amount of substance needed = 10 mM \* 10 mL =  $1.0 \cdot 10^{-4}$  mole

Thus,  $1.0 \cdot 10^{-4}$  mole of each pharmaceutical was weighed out to get a concentration of 10 mM in 10 mL of methanol. The amount which had to be weighed out for rapamycin and verapamil was also calculated following the calculation presented above, only as end concentration 1 mM was filled in. Every pharmaceutical was diluted in methanol, except for fenbendazole and albendazole, these were diluted in DMSO. The formed stock solutions were subsequently diluted in 5% ACN (0.1% FA) in  $H_2O$  (0.1% FA) via 2 steps to form a concentration of 10  $\mu M$  in 2 mL. First, 0.01 mL of the stock solution (10 mM in 10 mL methanol) was diluted in 0.99 mL of 5% ACN (0.1% FA) in  $H_2O$  (0.1% FA) giving a molarity of 100  $\mu M$ . Subsequently, 0.2 mL of the 100  $\mu M$  solution was diluted in 1.8 mL of 5% ACN (0.1% FA) in  $H_2O$  (0.1% FA) giving a molarity of 10  $\mu M$  in 2 mL. Rapamycin and Verapamil were diluted in 1 step to get to a concentration of 10  $\mu M$  in 2 mL. This was done by diluting 0.02 mL of the stock solution in 1.98 mL of 5% ACN (0.1% FA) in  $H_2O$  (0.1% FA) giving a molarity of 10  $\mu M$ . Afterwards, the diluted samples were put in autosampler vial micro inserts with a volume of 150  $\mu L$ .

### Oxidation of samples in electrochemical cell

All electrochemical measures were performed with an Antec ROXY potentiostat. The electrochemical reactions were performed in a Antec  $\mu$ -Prepcell, which is a one-compartment three-electrode cell in which the working electrode was either glassy carbon or platinum. Furthermore, the reference electrode was a Pd electrode, and the counter electrode was a carbonized PEEK electrode. Electrochemical measurements were performed with 3 different methods for which each 16 samples were used:

Method 1) 20  $\mu\text{L}$  of a 10  $\mu\text{M}$  sample was injected into the cell via the autosampler with a flow rate of 100  $\mu\text{L}/\text{min}$  of  $\text{H}_2\text{O}$  (0.1% FA) and ACN (0.1% FA). The potential was set to 1.5 V and the working electrode was glassy carbon.

Method 2) 5  $\mu\text{L}$  of  $\text{H}_2\text{O}_2$  (30 wt%) was added to the 150  $\mu\text{L}$  samples in the autosampler vial micro inserts, corresponding to circa 1 wt%  $\text{H}_2\text{O}_2$  in the total sample. This was subsequently mixed by pipetting the sample a couple of times up and down. Afterwards, 20  $\mu\text{L}$  of the sample was injected into the cell via the autosampler with a flowrate of 100  $\mu\text{L}/\text{min}$  of  $\text{H}_2\text{O}$  (0.1% FA) and ACN (0.1% FA). The potential was set to 1.5 V and the working electrode was Platinum.

Method 3) 20  $\mu\text{L}$  of 10  $\mu\text{M}$  sample was injected into the cell via the autosampler with a flowrate of 100  $\mu\text{L}/\text{min}$  of  $\text{H}_2\text{O}$  (0.1% FA) and ACN (0.1% FA). The potential was set to 2.5 V and the working electrode was glassy carbon.

The samples, which had just flown through the cell, were collected in 1.5 mL Eppendorf tubes with a time frame of 35 seconds to 105 seconds after being injected by the autosampler. This was done for all 15 samples with the 3 different methods. All collected samples were dried in an Eppendorf Concentrator Plus at a temperature of 60 degrees Celsius for approximately 45 minutes. The dried products were dissolved again in 80  $\mu\text{L}$  of 5% ACN (0.1% FA) in  $\text{H}_2\text{O}$  (0.1% FA) resulting in a calculated end concentration of 2.5  $\mu\text{M}$  of the combined compound and products.

### LC-MS analysis of collected samples

The potential metabolites present in the collected samples were qualified using LC-MS as seen in figure 3. The LC-MS consisted of a Shimadzu HPLC with LC 20AD XR binary pumps, SIL-30 ACMP autosampler and CTO-20A column oven for separation coupled to a Thermo Scientific TSQ quantum ultra-mass spectrometer. The compounds were separated on a reversed-phase C8 column (Waters XBridge columns; 2.1x150 mm) with a temperature of 40 degrees Celsius at a flow rate of 0.2 mL/min. The mobile phase consisted out of solvent A ( $\text{H}_2\text{O}$  with 0.1%FA) and solvent B (ACN with 0.1% FA). 20  $\mu\text{L}$  of the diluted pharmaceutical mixture was injected while a linear gradient was applied from 5 to 50% B over 8 minutes, followed by a fast increase to 95% B. This was held for 1 minute followed by an instant decline to 5% B for the last minute. Before any of the pharmaceuticals were oxidized following a certain method, a methanol blank was performed first. Mass spectra were recorded by electrospray ionization in positive mode, except for Salicylic acid which was recorded in a negative mode. Masses from  $m/z$  50 to 1000 were recorded. Chromatograms and mass spectra were recorded for 10 minutes. The data was processed in the Xcalibur software (Thermo Scientific).

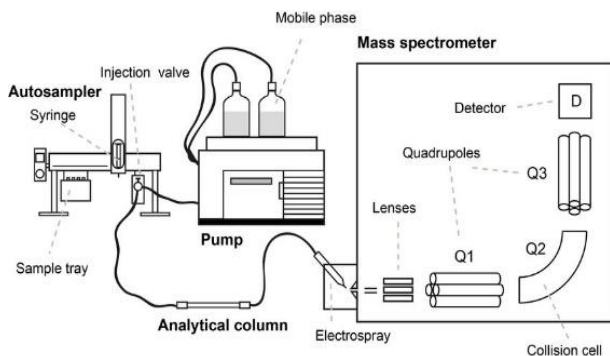


Figure 3: schematic overview of a LC/MS system [25].

## Data analysis

The data in Xcalibur presented both the chromatogram and mass spectrum of a chosen sample under a certain condition on the same screen. To give an illustration on how the data was analyzed, an example of the analysis of benztropine following method 2 (see table 2; page 13) is given. Figure 4 shows an overview of the chromatogram and mass spectrum of benztropine recorded for 10 minutes.

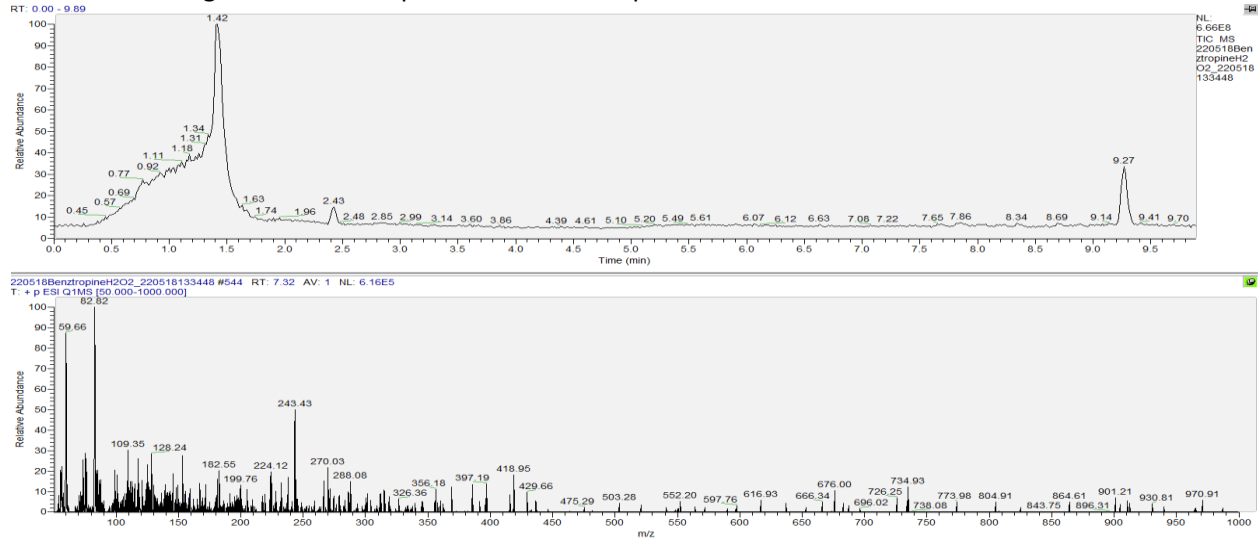


Figure 4: presented chromatogram (top) and mass spectrum (bottom) of benztropine under condition 2.

To see whether the pharmaceutical itself or expected metabolite(s) were detected by the LC/MS, the mass range was adjusted to the mass of this specific compound. When peaks in the chromatogram were found while using this tool, the found peaks were selected again and there was looked at the belonging mass spectrum. Figure 5 shows the peaks in the chromatogram which appeared after the mass range of 4-hydroxybenztropine, an expected metabolite of benztropine, was filled in. These found peaks were selected again and there was looked whether the belonging mass spectrum showed a peak at the correct m/z. Figure 5 shows a peak at 324.19 representing 4-hydroxybenztropine. This same method, explained above, was also done to find other expected metabolites or the pharmaceutical itself.

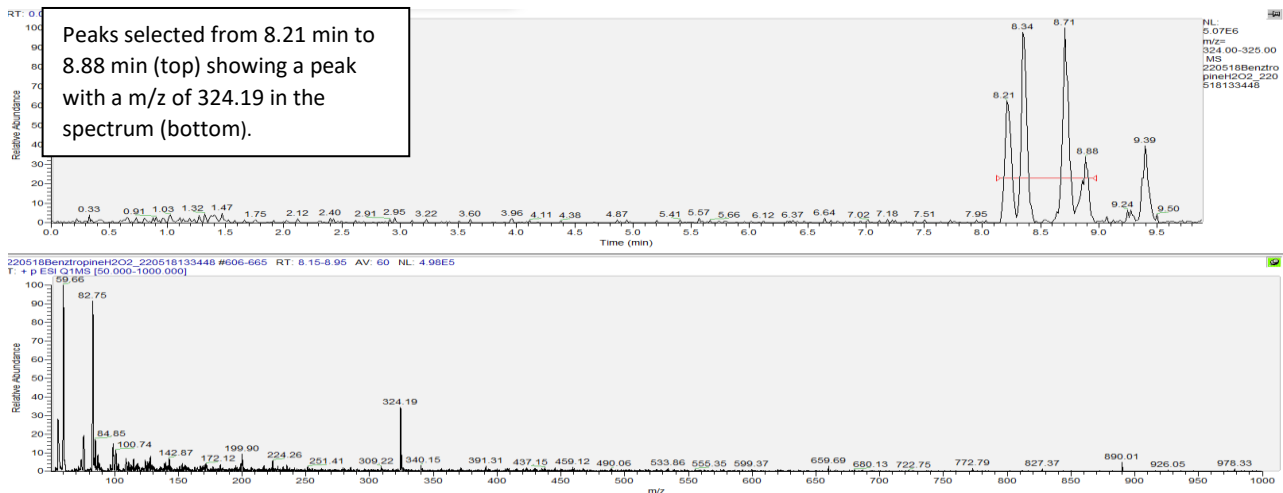


Figure 5: presented chromatogram (top) and mass spectrum (bottom) of benztropine under condition 2, in which the peaks in the chromatogram (found via the mass range tool) are selected showing the corresponding mass spectrum.

To confirm that the found oxidative metabolites were detected at a different retention time than the pharmaceutical, the mass ranges of both the metabolite and pharmaceutical were filled in. This resulted in two chromatograms, one chromatogram showing the peaks belonging to the mass range of the expected metabolite and the other chromatogram showing the peak belonging to the mass range of the pharmaceutical, as seen in figure 6.

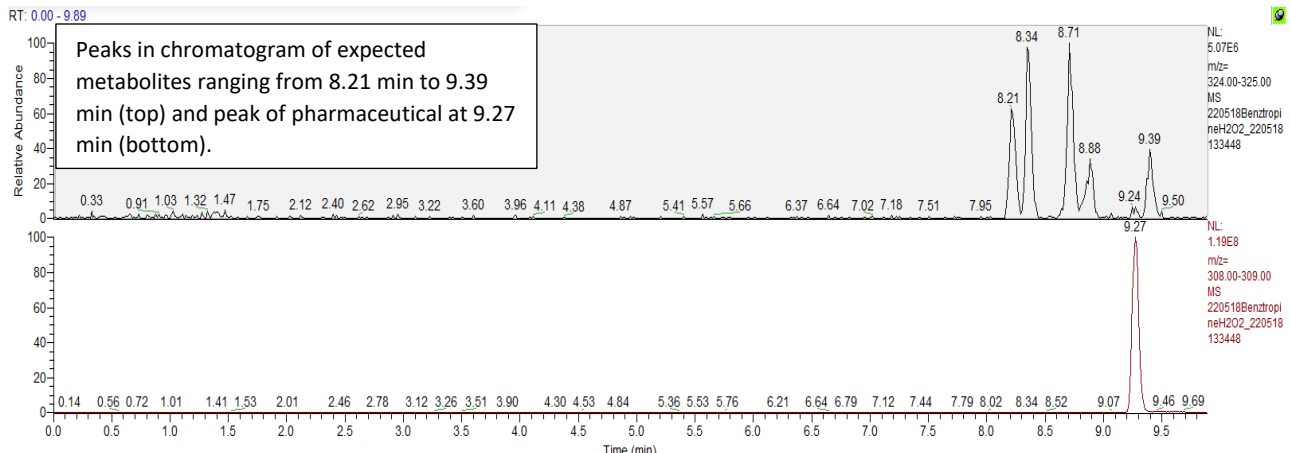


Figure 6: Chromatogram of benztropine found via the mass range of the expected metabolite (top) and a chromatogram of benztropine found via the mass range of the pharmaceutical itself (bottom).

When the found metabolite indeed had a different retention time than the pharmaceutical, there was assumed that a metabolite was formed in the electrochemical cell. Subsequently, the peaks in the chromatogram of both the metabolite and pharmaceutical were selected and the intensity of the peaks in the mass spectrum with the corresponding m/z were put in excel. This was done for all pharmaceuticals and their formed metabolites. Subsequently, the found intensities of each pharmaceutical per method were normalized to a total of 100%. Meaning that the intensity of the precursor and the intensities of the found metabolite(s) were summed up forming the total intensity (100%). Afterwards, the percentage of formed metabolite was calculated via formula 1:

$$[1] \text{ Formed metabolite (\%)} = (\text{Intensity of metabolite} / \text{total intensity}) * 100\%$$

This calculation was done for every pharmaceutical under each condition were possible. The calculated percentages were subsequently put in a bar chart. The conversion rates of the pharmaceuticals were also calculated. This was done by summing up the percentage of formed metabolites per pharmaceutical under each condition. The found conversion rates were also put in a table.

## Results and Discussion

### The different conditions

During this study the extent to which electrochemistry can mimic *in vivo* phase 1 metabolism of various pharmaceuticals was investigated. The pharmaceuticals were oxidated under various conditions to enlarge the chance of *in vivo* phase 1 metabolites being formed with electrochemistry. The 3 different conditions in the electrochemical cell can be seen in table 2. According to literature, the most crucial EC parameters for oxidation of pharmaceuticals are potential, pH, electrode type and substrate concentration. Meaning that these parameters must be varied to create beneficial opportunities for oxidative metabolites to be formed and thus to successfully mimic *in vivo* phase 1 metabolism. However, due to time limitations during this study to do practical work, there was chosen to vary two of the above stated parameters. For these 3 different conditions, the electrode type and potential were varied. Glassy carbon is a widely known and used electrode type with various advantages, therefore this type was chosen as electrode type for condition 1 and 3. The parameter varying between condition 1 and 3 is the potential, in which condition 1 uses a potential of 1.5 V and condition 3 of 2.5 V. A potential of 1.5 V is chosen since literature supports that this potential results in a high amount of oxidation [26]. The potential of condition 3 is increased by 1 V with the aim of investigating whether the higher amount of energy, supplied by a higher potential, results in more oxidation reactions to happen. Condition 2 uses H<sub>2</sub>O<sub>2</sub> together with a platinum electrode to generate reactive oxygen species (ROS) via electrocatalytic oxidation of hydrogen peroxide. These formed ROS are capable of oxygen-insertion reactions like CYP450s can do at their active site [27]. Thus, with this method, it is expected that *in vivo* oxidative drug metabolism, specifically hydroxylation, can be mimicked with EC.

Table 2: representation of the three different conditions used to study the ability of EC to mimic *in vivo* phase 1 metabolism.

| Method | Electrode type | Potential | Extra  |
|--------|----------------|-----------|--|
| 1      | Glassy carbon  | 1.5 V     |  |
| 2      | Platinum       | 1.5 V     | 5 $\mu$ L of H <sub>2</sub> O <sub>2</sub> added |
| 3      | Glassy carbon  | 2.5 V     |  |

### Pharmaceuticals without oxidative metabolites

From the panel of pharmaceuticals used for these experiments, there are 5 pharmaceuticals which did not show any oxidative metabolites in the LC-MS spectra. For rapamycin, coumarin, atropine, caffeine and salicylic acid no oxidative metabolites were found in all 3 three methods. The compound coumarin itself was also not detected by the LC-MS, whereas it was detected when testing the LC-MS without an electrochemical cell. This could mean that all of the injected coumarin was oxidized in the electrochemical cell under every condition. However, since no metabolite is found under any condition with the electrochemical cell, the likelihood of this being the reason for no detection of coumarin is nil. A reason which could explain the absence of any detection of coumarin, or its metabolite is that coumarin was fully converted into its intermediate coumarin 3,4-epoxide, which subsequently reacted with other intermediates forming oligomers. These oligomers have a high molecular weight which could have resulted in the oligomers not coming off the LC column and thus not being detected by the MS [28]. The rest of the pharmaceuticals, which did not show any oxidative metabolites, did were detected themselves by the LC-MS. The fact that no oxidative metabolites were detected for these 5 pharmaceuticals is probably since the EC conditions, under which these experiments were performed,

were not optimal, specifically for these pharmaceuticals. Therefore, it is essential that optimal conditions are used when doing such an experiment. However, during this study only three different types of conditions were used to try and mimic in vivo metabolism. This leads to a viable chance that the optimal condition was not met for a certain number of pharmaceuticals resulting in no oxidation. The fact that no hydroxylated products of salicylic acid, coumarin and rapamycin were found under condition 2 is therefore also probably caused by the fact that other parameters in the electrochemical cell were not optimized for these pharmaceuticals.

### Pharmaceuticals with dealkylated in vivo metabolites

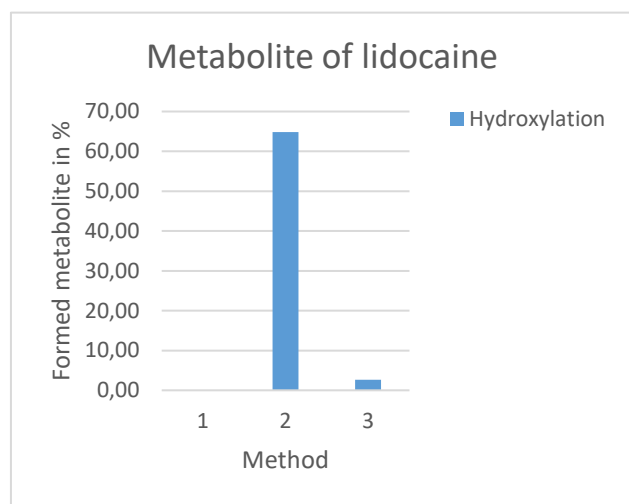


Figure 7: bar chart of lidocaine showing the % of formed metabolite under each condition.

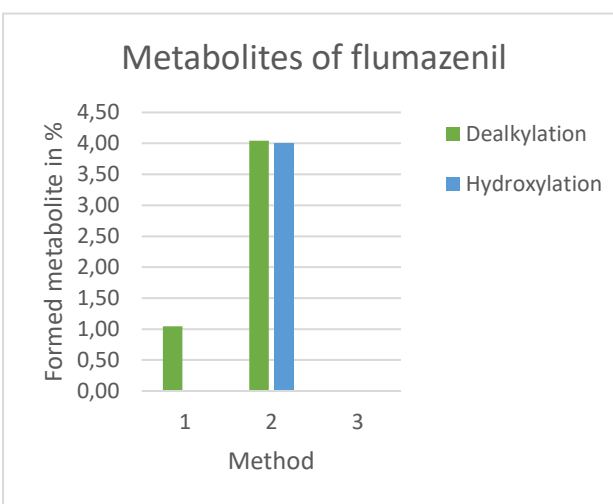


Figure 8: bar chart of flumazenil showing the % of formed metabolite under each condition.

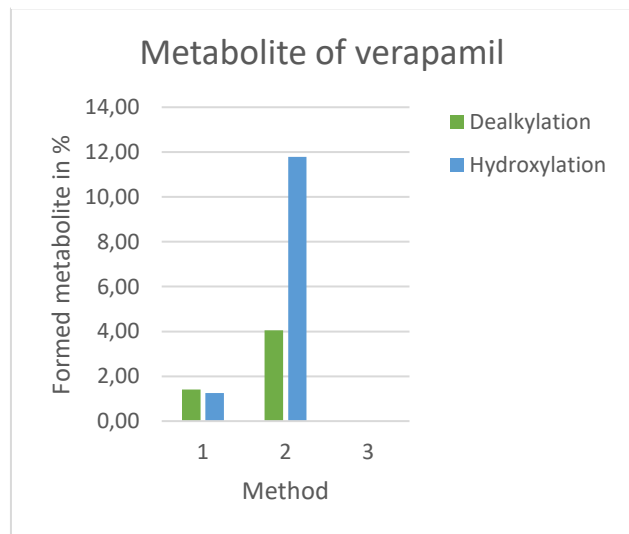


Figure 9: bar chart of verapamil showing the % of formed metabolite under each condition.

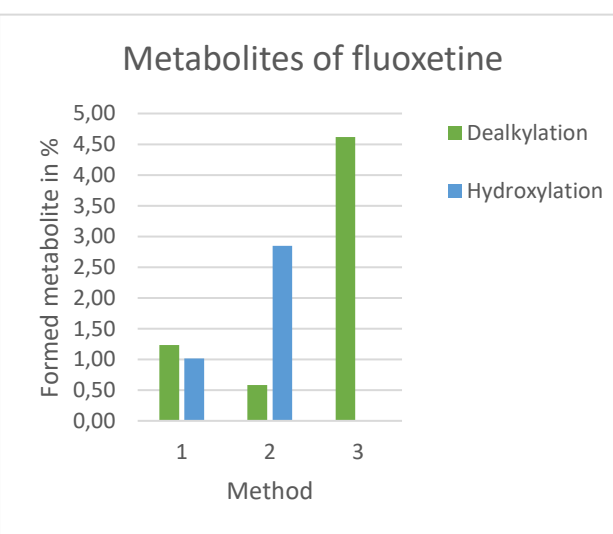


Figure 10: bar chart of fluoxetine showing the % of formed metabolite under each condition.

Lidocaine, flumazenil, verapamil, and fluoxetine all have a similar in vivo oxidation pattern. According to literature, these four pharmaceuticals are all dealkylated during phase 1 metabolism, thereby enhancing the polarity of the compound. Therefore, the known in vivo metabolites of these pharmaceuticals are MEGX, GX, N-desmethyl flumazenil, norverapamil and norfluoxetine. When looking at figures 7 to 10, it can be seen that the type of oxidation reaction and the optimal condition varied among these pharmaceuticals. The in vivo metabolites of lidocaine are MEGX and GX, where MEGX is the once de-ethylated form of lidocaine and GX is the twice de-ethylated form of lidocaine. However, in the mass spectra no peaks were found with either a mass loss of 28 or 56 with respect to lidocaine itself. Meaning that no dealkylated product was formed and thus that no in vivo metabolite was formed. However, figure 7 does show that a hydroxylated product was formed under condition 2 and 3, in which the amount of hydroxylated product under condition 2 is significantly higher than under condition 3. Yet, lidocaine is not hydroxylated by CYP450s during phase 1 metabolism and thus are the found hydroxylated product no in vivo metabolites.

Flumazenil, verapamil, and fluoxetine all showed a similar oxidation pattern in the electrochemical cell, namely that these pharmaceuticals were both hydroxylated and dealkylated. For all pharmaceuticals a peak was found in the mass spectrum with a mass loss of 14 with respect to the pharmaceutical itself. The mass loss of 14 implies the extraction of 1 carbon atom and 2 hydrogen atoms which indicates demethylation and thus dealkylation. The formed dealkylated products of the three pharmaceuticals are all expected in vivo metabolites namely, N-demethylated flumazenil, norfluoxetine and norverapamil. When looking at figures 8 to 10, it can be seen that the amount of dealkylated product formed differs per condition for each pharmaceutical. For flumazenil and verapamil, method 2 resulted in the most dealkylated metabolite, whereas method 3 formed the most dealkylated product for fluoxetine. However, when looking at the y-axis it can be seen that the differences between the three different conditions for the amount of formed dealkylated product is not significant (namely 0 to 5% difference). Therefore, the parameters varied in the three different conditions do not have a major influence on the rate of dealkylation for these 3 pharmaceuticals.

Furthermore, a peak in the mass spectrum with a mass gain of 16 was also found for flumazenil, verapamil and fluoxetine as seen in figures 8 to 10. For all pharmaceuticals the amount of hydroxylated product formed was the highest under condition 2. This was expected, since condition 2 used H<sub>2</sub>O<sub>2</sub> combined with a platinum electrode, thereby forming ROS which stimulates oxygen insertion reactions and thus hydroxylation. Nonetheless, flumazenil, fluoxetine and verapamil are not hydroxylated in vivo by CYP450s during phase 1 metabolism and thus are the found hydroxylated products for these pharmaceuticals not known in vivo metabolites.

It can be stated that condition 2 is the most optimal condition for flumazenil and verapamil to mimic in vivo phase 1 metabolism as this condition forms the known in vivo metabolites with the highest yields. Whereas condition 3 is the most beneficial when wanting to mimic the in vivo metabolism of fluoxetine. For lidocaine none of the three conditions is optimal since no in vivo metabolite was found under all three conditions.

## Pharmaceuticals with hydroxylated in vivo metabolites

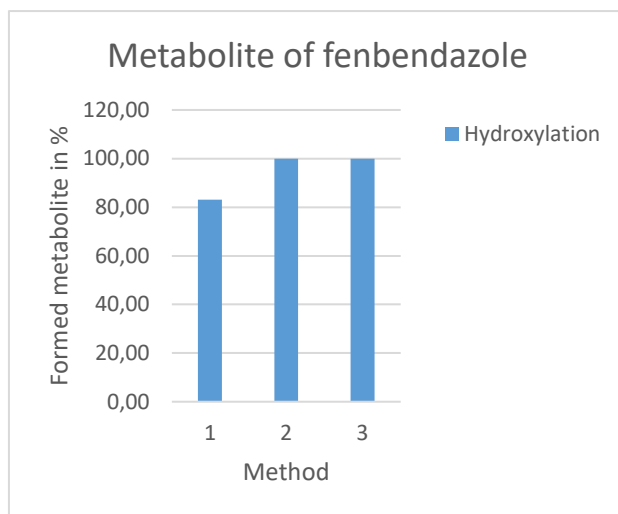


Figure 11: bar chart of fenbendazole showing the % of formed metabolite under each condition.

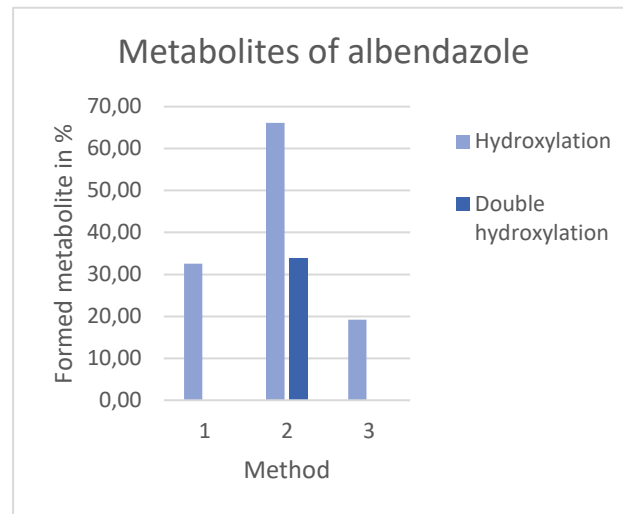


Figure 12: bar chart of albendazole showing the % of formed metabolite under each condition.

Fenbendazole and albendazole are both hydroxylated during in vivo phase 1 metabolism, thereby forming 4-hydroxyfenbendazole and 8-hydroxyalbendazole. For both pharmaceuticals peaks with a mass gain of 16 were found in the mass spectra, implying that an oxygen atom was introduced to the molecules forming a hydroxyl group. However, a mass gain of 16 could also indicate the formation of a sulfoxide, which is a plausible option when looking at the structure of fenbendazole and albendazole. Yet, since the known in vivo metabolites are a hydroxylated form of the pharmaceuticals, it can be assumed that the mass gain of 16 implies a hydroxy metabolite and not a sulfoxide metabolite. To assure that no sulfoxide metabolite was formed, more experiments need to be conducted.

A remarkable thing which can be seen in both figures, it that the conversion rate for these pharmaceuticals is surprisingly high compared to the previously discussed pharmaceuticals. Figure 11 shows that the amount of metabolite formed under condition 2 and 3 are both 100%, meaning that everything of fenbendazole is oxidized into the metabolite. This conversion rate is this high because no fenbendazole was detected by the LC/MS, like what happened to coumarin. However, a difference between fenbendazole and coumarin is that metabolites of fenbendazole were found with high intensities under these conditions, whereas this was not the case for coumarin. This suggest that there was a full conversion of fenbendazole into 4-hydroxyfenbedazole. With method 1, a lower conversion rate is seen, because still some unoxidized fenbendazole was detected under this condition. The conversion rate of albendazole is lower than fenbendazole but also significantly higher than the previous mentioned pharmaceuticals as seen in figure 12. The amount of formed 8-hydroxyalbendazole is again the highest under condition 2 due to the stimulation of oxygen insertion. Additionally, a peak was recognized in the spectrum of method 2 with a mass gain of 32 with respect to albendazole. This suggests that a part of albendazole was double hydroxylated, which is possible. The hydrogen peroxide was present in a solution thereby making it able for the ROS to surround the molecule and thus hydroxylate the molecule on different sites. Double hydroxylation does however not form an in vivo metabolite since the CYP450s are more specific due to their hydrophobic pocket which can only bind to and thereby hydroxylate a certain part of the molecule.



Thus, the in vivo phase 1 metabolism of fenbendazole and albendazole was successfully mimicked. For fenbendazole, condition 2 and 3 are the most optimal since here all the fenbendazole is converted into its known in vivo metabolite. Condition 2 also achieves the highest conversion rate of albendazole and is therefore the most optimal condition for albendazole.

## Pharmaceuticals with dealkylated and hydroxylated in vivo metabolites

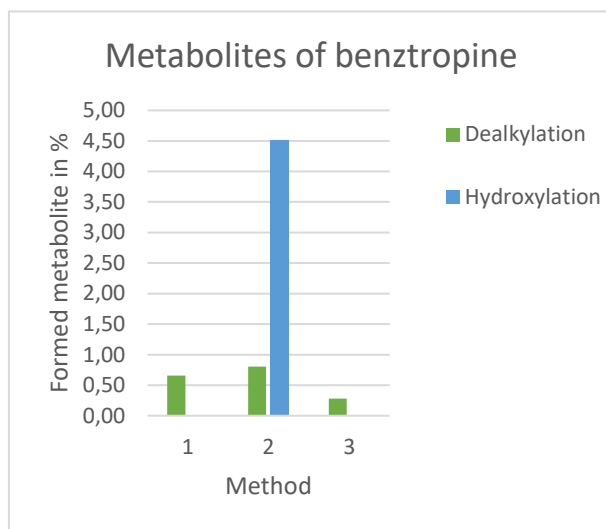


Figure 13: bar chart of benztropine showing the % of formed metabolite under each condition.

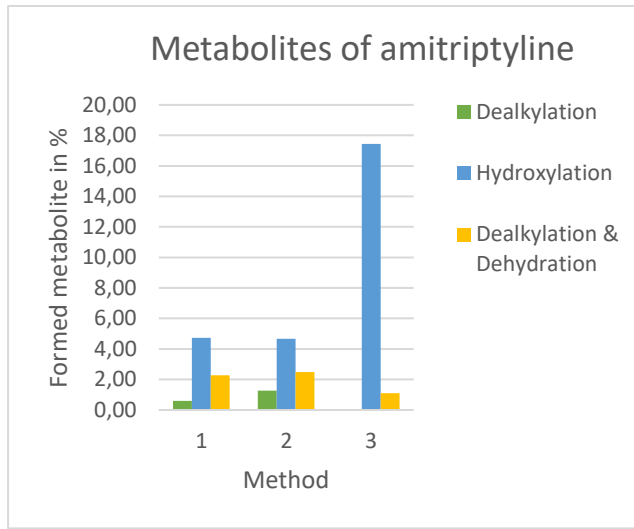


Figure 14: bar chart of amitriptyline showing the % of formed metabolite under each condition.

Benztropine and amitriptyline are both either dealkylated or hydroxylated during in vivo phase 1 metabolism thereby forming N-desmethylbenztropine, 4-hydroxy benztropine, nortriptyline and 10-hydroxy amitriptyline. Figures 13 and 14 show that for both pharmaceuticals the dealkylated product as well as the hydroxylated product were detected by the LC/MS under different conditions. Benztropine was converted into the in vivo metabolite N-desmethylbenztropine under all three conditions, whereas amitriptyline was converted into nortriptyline under condition 1 and 2. Even though the dealkylated in vivo metabolite is formed in the electrochemical cell, the yields for both pharmaceuticals are certainly low.

Furthermore, both pharmaceuticals were hydroxylated into their in vivo phase 1 metabolite 4-hydroxy benztropine or 10-hydroxy amitriptyline. Benztropine was only hydroxylated under condition 2 which is because this condition used  $H_2O_2$  and a platinum electrode, thereby forming ROS stimulating hydroxylation. Amitriptyline was hydroxylated under all 3 conditions, in which condition 3 resulted in the highest amount of hydroxylated metabolite to be formed. This is surprising since this method did not use hydrogen peroxide and a platinum electrode to stimulate this oxidative reaction. Lastly, peaks with a mass loss of 16 with respect to amitriptyline itself were found in the MS spectrum for all methods. This suggests that amitriptyline was both demethylated and dehydrated in the electrochemical cell thereby forming nortriptyline with an extra double bond present in the molecule. This product is however not an in vivo phase 1 metabolite.

Hence, both the expected in vivo phase 1 metabolites of benztropine and amitriptyline were formed. For benztropine condition 2 is the most favorable condition since this leads to the formation of both in vivo metabolites with the highest yields. Condition 3 did lead to the highest rate of hydroxylation of amitriptyline, however, did not result in any dealkylated metabolite being formed. Therefore condition 1 or 2 should be used to mimic the in vivo phase 1 metabolism of amitriptyline since these conditions formed both in vivo metabolites, however with a low yield.

### Pharmaceuticals with dealkylated and N-/S-oxidized in vivo metabolites

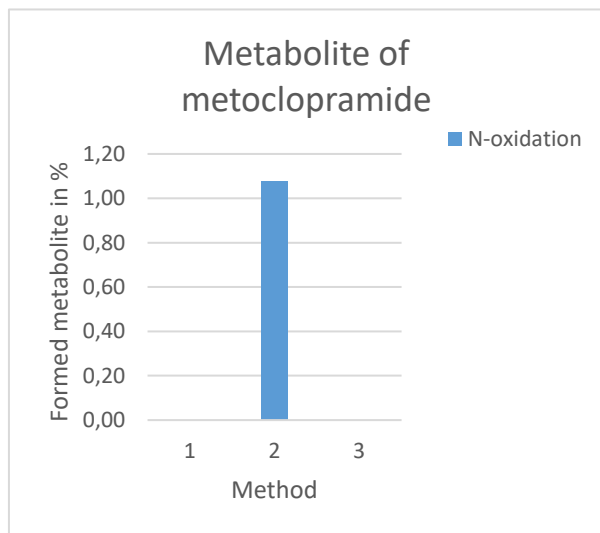


Figure 15: bar chart of metoclopramide showing the % of formed metabolite under each condition.

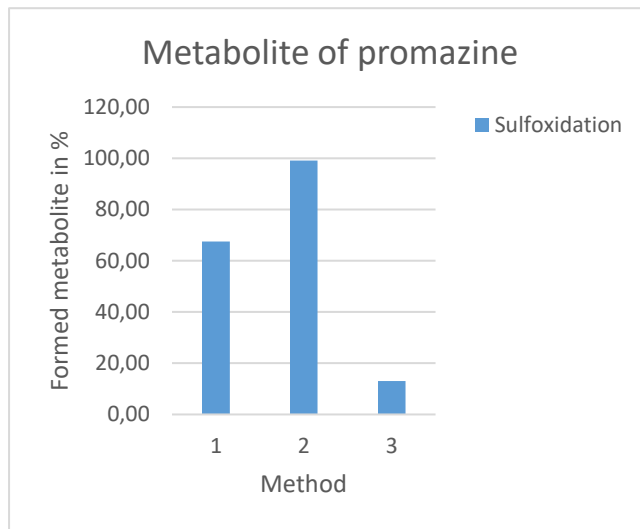


Figure 14: bar chart of promazine showing the % of formed metabolite under each condition.

Metoclopramide and promazine are dealkylated during in vivo phase 1 metabolism, thereby forming N-de-ethylated metoclopramide and N-desmethylpromazine. Furthermore, they are also both metabolized via oxidation of the hetero atoms nitrogen or sulfur, where the nitrogen atom in metoclopramide is oxidized forming mono-oxygenated metoclopramide and where the sulfur atom of promazine is oxidized (sulfoxidation) forming promazine sulfoxide. For both pharmaceutical a peak with a mass gain of 16 was found in the mass spectra, indicating the binding of an oxygen atom to the compound. For the previous pharmaceuticals, a mass gain of 16 was assumed to be hydroxylation, since the expected in vivo metabolites contain a hydroxyl group. However, since the expected in vivo metabolites of metoclopramide and benztropine rely on the oxygen to bind to either nitrogen or sulfur, it is assumed that the mass gain of 16 implies N-oxidation and sulfoxidation. Figure 15 shows that N-oxidation only happened under condition 2, which is not surprising since this method used ROS to stimulate the oxygen insertion. The fact that under condition 1 and 3 no oxidation metabolite was formed suggests that the potential does not influence the N-oxidation of metoclopramide. As seen in figure 16, promazine sulfoxide is formed under all three conditions, where the conversion rates of condition 1 and 2 are high. The dealkylated in vivo phase 1 metabolites of both pharmaceuticals were not formed under these conditions.

Thus, a favorable condition for the mimicry of in vivo phase 1 metabolism of metoclopramide and promazine is not yet found, since no condition forms both the expected in vivo metabolites.

Table 3: representation of the calculated conversion rates for the pharmaceuticals under each condition. \*N.D. stands for non-detectable.

| Pharmaceutical | Conversion rate method 1 | Conversion rate method 2 | Conversion rate method 3 |
|----------------|--------------------------|--------------------------|--------------------------|
| Rapamycin      | 0.00                     | 0.00                     | 0.00                     |
| Atropine       | 0.00                     | 0.00                     | 0.00                     |
| Coumarin       | N.D.                     | N.D.                     | N.D.                     |
| Benztropine    | 0.66                     | 5.3                      | 0.28                     |
| Caffeine       | 0.00                     | 0.00                     | 0.00                     |
| Flumazenil     | 0.00                     | 4.0                      | 0.00                     |
| Fluoxetine     | 2.3                      | 3.4                      | 4.6                      |
| Fenbendazole   | 83.1                     | 100.0                    | 100.0                    |
| Amitriptyline  | 7.6                      | 8.4                      | 18.5                     |
| Metoclopramide | 0.00                     | 1.1                      | 0.00                     |
| Lidocaine      | 0.00                     | 64.9                     | 2.6                      |
| Albendazole    | 32.5                     | 100.0                    | 19.2                     |
| SA             | 0.00                     | 0.00                     | 0.00                     |
| Promazine      | 67.5                     | 99.1                     | 13.1                     |
| Verapamil      | 2.7                      | 15.8                     | 0.00                     |

In table 3, the conversion rates of the various pharmaceuticals for the three conditions can be seen. As already stated before, rapamycin, atropine, caffeine, and salicylic acid all have a conversion rate of 0% as a result of no formation of oxidative metabolites. N.D. stated in the column of coumarin implies that both the precursor and product were not detectable and thus that no conversion rate could be calculated for this compound. Besides these pharmaceuticals, the other pharmaceuticals have a calculated conversion rate for most of the conditions.

When having a global look at the table, one can see that the conversion rate under condition 2 is in most cases higher than under the other conditions for the pharmaceuticals. This is caused by hydrogen peroxide and the platinum electrode acting like a catalyst for oxygen insertion reactions. This also means that most metabolites under condition 2 are formed via hydroxylation, oxidation or sulfoxidation since these reactions rely on an oxygen atom to be inserted in the molecule. The previously mentioned phenomenon can also be seen in the figures stated above in the results, where the amount of formed metabolite via oxygen-insertion reactions is in most cases higher than metabolites formed via, for example, dealkylation under condition 2. Therefore, condition 2, forming frequently metabolites via oxygen-insertion reactions, is favorable to mimic in vivo phase 1 metabolism when expecting a metabolite via hydroxylation, sulfoxidation or oxidation. When a dealkylated product is expected as a metabolite, condition 2 also gives the highest conversion rate in most cases. However, there are also cases in which dealkylated metabolites are expected and in which condition 2 subsequently only gives unwanted hydroxylated metabolites. Thus, a consideration must be made whether to use condition 2 for pharmaceuticals with in vivo dealkylated metabolites. Furthermore, it was expected that a higher potential results in a higher conversion rate since more energy is available to make these reactions happen. However, when looking at the figures displayed in the results, occasionally the conversion rate of a pharmaceutical is higher under condition 1 and occasionally it is higher under condition 3. Therefore, the influence of potential on the formation of metabolites is not significant when using a glassy carbon electrode.

Since the in vivo phase 1 metabolism is not mimicked successfully for every pharmaceutical, a recommendation for a future study could be to try and mimic this successfully under different conditions. For this study only three different conditions were tested, in which the electrode type and potential were varied. To successfully mimic the metabolism performed by the CYP450 system for the other pharmaceuticals, more parameters like pH, flow rate and substrate concentration should be varied and divided over separated conditions. By using a bigger variety of different conditions, the chance of successfully mimicking in vivo phase 1 metabolism of these pharmaceuticals will increase. In the figures displayed in the results and in table 3, it can also be seen that the yields of most formed in vivo metabolites are low. Therefore, another recommendation for a future study could be to increase the yields of the formed in vivo oxidative metabolites. This can be done by using a batch cell for the electrochemical measurements so that the pharmaceuticals are longer in contact with the electrode surface resulting in more oxidation and thus a higher yield of the metabolites.

## Conclusion

Based on the data presented above, one can conclude that the in vivo phase 1 metabolism was successfully mimicked for 7 pharmaceuticals. Thus, by performing EC/LC/MS, in vivo metabolites were formed and detected for these 7 pharmaceuticals. Occasionally a hydroxylated metabolite was found besides the corresponding in vivo metabolite(s) for a certain pharmaceutical. This was only seen under condition 2 and was thus caused by the hydrogen peroxide and platinum electrode catalyzing this reaction. For 2 pharmaceuticals only one of the two in vivo phase 1 metabolites was found. For both pharmaceuticals the metabolite formed through either sulfoxidation, or N-oxidation was found, while the N-dealkylated form was not formed. For 6 pharmaceuticals, no corresponding in vivo metabolites were found. Overall, it can be concluded that the in vivo phase 1 metabolism was mimicked successfully via EC for almost half of the chosen pharmaceuticals, whereas other conditions must be applied to successfully mimic the in vivo phase 1 metabolism of the other pharmaceuticals.

## References

1. Singh, S. (2006). Preclinical Pharmacokinetics: An Approach Towards Safer and Efficacious Drugs. *Current Drug Metabolism*, 7(2), 165–182. <https://doi.org/10.2174/138920006775541552>
2. Bachmann, K. (2009). Drug metabolism. *Book Pharmacology*.
3. Almazroo, O.A., Miah, M.K., Venkataramanan, R. (2017). Drug metabolism in the liver. *Clinics in Liver Disease*, 21(1), 1-20. <https://doi.org/10.1016/j.cld.2016.08.001>
4. Šrejber, M., Navrátilová, V., Paloncýová, M., Bazgier, V., Berka, K., Anzenbacher, P., & Otyepka, M. (2018). Membrane-attached mammalian cytochromes P450: An overview of the membrane's effects on structure, drug binding, and interactions with redox partners. *Journal of Inorganic Biochemistry*, 183, 117–136. <https://doi.org/10.1016/j.jinorgbio.2018.03.002>
5. Nouri-Nigjeh, E., Bischoff, R., P. Bruins, A., & P. Permentier, H. (2011). Electrochemistry in the Mimicry of Oxidative Drug Metabolism by Cytochrome P450s. *Current Drug Metabolism*, 12(4), 359–371. <https://doi.org/10.2174/138920011795202929>
6. Shankar, K., Menhendale, H.M. (2014). Cytochrome P450. *Encyclopedia of Toxicology*, 26-29.
7. Belcher, J., McLean, K. J., Matthews, S., Woodward, L. S., Fisher, K., Rigby, S. E., Nelson, D. R., Potts, D., Baynham, M. T., Parker, D. A., Leys, D., & Munro, A. W. (2014). Structure and Biochemical Properties of the Alkene Producing Cytochrome P450 OleTJE (CYP152L1) from the *Jeotgalicoccus* sp. 8456 Bacterium. *Journal of Biological Chemistry*, 289(10), 6535–6550. <https://doi.org/10.1074/jbc.m113.527325>
8. Bussy, U., Delaforge, M., El-Bekkali, C., Ferchaud-Roucher, V., Krempf, M., Tea, I., Galland, N., Jacquemin, D., & Boujtita, M. (2013a). Acebutolol and alprenolol metabolism predictions: comparative study of electrochemical and cytochrome P450-catalyzed reactions using liquid chromatography coupled to high-resolution mass spectrometry. *Analytical and Bioanalytical Chemistry*, 405(18), 6077–6085. <https://doi.org/10.1007/s00216-013-7050-7>
9. Patel, B.A. (2020). Introduction to electrochemistry for bioanalysis. *Electrochemistry for Bioanalysis*, 1-8.
10. Lohmann, W., Dötzer, R., Gütter, G., Van Leeuwen, S. M., & Karst, U. (2009). On-line electrochemistry/liquid chromatography/mass spectrometry for the simulation of pesticide metabolism. *Journal of the American Society for Mass Spectrometry*, 20(1), 138–145. <https://doi.org/10.1016/j.jasms.2008.09.003>
11. Bojić, M., Sedgeman, C. A., Nagy, L. D., & Guengerich, F. P. (2015). Aromatic hydroxylation of salicylic acid and aspirin by human cytochromes P450. *European Journal of Pharmaceutical Sciences*, 73, 49–56. <https://doi.org/10.1016/j.ejps.2015.03.015>
12. Vassallo, J. D., Hicks, S. M., Daston, G. P., & Lehman-McKeeman, L. D. (2004). Metabolic Detoxification Determines Species Differences in Coumarin-Induced Hepatotoxicity. *Toxicological Sciences*, 80(2), 249–257. <https://doi.org/10.1093/toxsci/kfh162>
13. BILL, T. (2004a). Lidocaine metabolism pathophysiology, drug interactions, and surgical implications. *Aesthetic Surgery Journal*, 24(4), 307–311. <https://doi.org/10.1016/j.asj.2004.05.001>
14. Yuan, T. (2017). *Nanostructured gold: applications in the study of drug metabolism*. University of Groningen.

15. Christians, U., Sattler, M., Schiebel, H.M., Kruse, C., Radeke, H.H., Linck, A., Sewing, K.F. (1992). Isolation of two immunosuppressive metabolites after in vitro metabolism of rapamycin. *Drug Metab Dispos*, 20(2), 186-191. PMID: 1352208.
16. Wu, Z., Lee, D., Joo, J., Shin, J. H., Kang, W., Oh, S., Lee, D. Y., Lee, S. J., Yea, S. S., Lee, H. S., Lee, T., & Liu, K. H. (2013). CYP2J2 and CYP2C19 Are the Major Enzymes Responsible for Metabolism of Albendazole and Fenbendazole in Human Liver Microsomes and Recombinant P450 Assay Systems. *Antimicrobial Agents and Chemotherapy*, 57(11), 5448–5456.  
<https://doi.org/10.1128/aac.00843-13>
17. Kleingeist, B., Bocker, R., Geisslinger, G., Brugger, R. (1998). Isolation and pharmacological characterization of microsomal human liver flumazenil carboxylesterase. *J Pharm Pharm Sci*, 1(1), 38-46. PMID: 10942971.
18. Tracy, T. S., Korzekwa, K. R., Gonzalez, F. J., & Wainer, I. W. (1999). Cytochrome P450 isoforms involved in metabolism of the enantiomers of verapamil and norverapamil. *British Journal of Clinical Pharmacology*, 47(5), 545–552. <https://doi.org/10.1046/j.1365-2125.1999.00923.x>
19. Livezey, M. R., Briggs, E. D., Bolles, A. K., Nagy, L. D., Fujiwara, R., & Furge, L. L. (2013). Metoclopramide is metabolized by CYP2D6 and is a reversible inhibitor, but not inactivator, of CYP2D6. *Xenobiotica*, 44(4), 309–319. <https://doi.org/10.3109/00498254.2013.835885>
20. Dean, L. (2017). Amitriptyline Therapy and CYP2D6 and CYP2C19 Genotype. *Medical Genetics Summaries*.
21. Thorn, C. F., Aklillu, E., McDonagh, E. M., Klein, T. E., & Altman, R. B. (2012). PharmGKB summary. *Pharmacogenetics and Genomics*, 22(5), 389–395.  
<https://doi.org/10.1097/fpc.0b013e3283505d5e>
22. Deodhar, M., Rihani, S. B. A., Darakjian, L., Turgeon, J., & Michaud, V. (2021). Assessing the Mechanism of Fluoxetine-Mediated CYP2D6 Inhibition. *Pharmaceutics*, 13(2), 148.  
<https://doi.org/10.3390/pharmaceutics13020148>
23. He, H., McKay, G., & Midha, K. K. (1995). Phase I and II metabolites of benzotropine in rat urine and bile. *Xenobiotica*, 25(8), 857–872. <https://doi.org/10.3109/00498259509061899>
24. Daniel, W., Syrek, M., Janczar, L., Boska, J. (1995) The pharmacokinetics of promazine and its metabolites after acute and chronic administration to rats—a comparison with the pharmacokinetics of imipramine. *Pol J Pharmacol*, 47(2), 127-136. PMID: 8688885.
25. Ostman, M. (2018). Antimicrobials in sewage treatment plans. DOI: 10.13140.
26. Gul, T., Bischoff, R., & Permentier, H. P. (2015). Optimization of reaction parameters for the electrochemical oxidation of lidocaine with a Design of Experiments approach. *Electrochimica Acta*, 171, 23–28. <https://doi.org/10.1016/j.electacta.2015.04.160>
27. Nouri-Nigjeh, E., Bischoff, R., P. Bruins, A., & P. Permentier, H. (2011). Electrochemistry in the Mimicry of Oxidative Drug Metabolism by Cytochrome P450s. *Current Drug Metabolism*, 12(4), 359–371. <https://doi.org/10.2174/138920011795202929>
28. Hsieh, C. J., Sun, M., Osborne, G., Ricker, K., Tsai, F. C., Li, K., Tomar, R., Phuong, J., Schmitz, R., & Sandy, M. S. (2019). Cancer Hazard Identification Integrating Human Variability: The Case of Coumarin. *International Journal of Toxicology*, 38(6), 501–552.  
<https://doi.org/10.1177/1091581819884544>